

Ab initio calculation of the thermal conductivity of InSb

Alonso L.Miranda^{1,2}, Bin Xu^{2,3}, Olle Hellman⁴, Aldo H.Romero^{1,5} and Matthieu J. Verstraete².

¹CINVESTAV, Departamento de Materiales, Unidad Querétaro, Querétaro, 76230, México

²Département de Physique, Université de Liège, Allée du 6 Août 17, B-400 Sart Tilman, Belgium

³Physics Department and Institute for Nanoscience and Engineering, University of Arkansas, Fayetteville, AR 72701, USA

⁴Department of Physics, Chemistry and Biology (IFM), Linköping University, SE-581 83, Linköping, Sweden

⁵Department of Physics and Astronomy, West Virginia University, WV-26506-6315, Morgantown, USA

Abstract. A theoretical study based on the Density Functional Theory and the temperature dependent effective potential method is performed to analyze the changes in the phonon band structure as function of temperature for InSb. In particular, we show changes in the thermal expansion coefficient and the thermal resistivity that agree rather well with experimental measurements. From the theoretical side, we show a weak dependence with respect to the chosen thermostat used to obtain the inter atomic force constants, which strengthens our conclusions.

1. Introduction

Thermal conductivity is a fundamental transport property that is commonly used to characterize materials, in particular for semiconductors as it becomes critical when we go to smaller length scales. High thermal conductivity materials are useful for passive heat dissipation, whereas low thermal conductivity is essential for highly efficient thermoelectric materials[1]. In semiconductors, the majority of the heat is carried by lattice vibrations (phonons) while the electronic contributions is negligible except at very low temperature[2].

Indium antimonide (InSb) is a narrow-gap semiconductor (0.18 eV at room temperature) with technological importance, which can be used in infrared detectors, thermal imaging cameras and in Shottky diodes. It has a very large electron mobility ($78000 \text{ cm}^2\text{V}^{-1}$) at room temperature [3], and it is a promising thermoelectric material among the III-V semiconductors [4]. The giant spin Seebeck effect was recently observed in InSb [5]. However, one critical limitation to improve the thermoelectric figure of merit ZT is the relatively high lattice thermal conductivity, e.g., 20W/mK at 300 K. The lattice thermal conductivity κ_l of InSb has been investigated experimentally in the range 1.7 to 300 K [6].

A predictive theoretical approach to calculate the lattice thermal conductivity in these materials becomes of great help if our purpose is to engineer some of the thermal properties that could improve the thermoelectric response. In this paper, the temperature dependence of thermal properties of crystalline InSb semiconductor is analyzed in detail.

2. Formalism

Calculations of the lattice vibration and thermal properties were carried out using the temperature dependent effective potential (TDEP) code as implemented by Hellman *et al* [7, 8]. The generalized TDEP uses a Hamiltonian expanded as a function of the ionic positions in harmonic and anharmonic (including the 3rd- and 4th-order) force constants, which are obtained by fitting the Born-Oppenheimer potential energy surface. The energy surface is sampled by using first principles ab initio molecular dynamics (AIMD) at a predefined temperature and volume and keeping the corresponding symmetries of the original crystal in place. This method has proven to provide very accurate phonon dispersion relations and free energies for large temperatures and in particular, where anharmonic effects become substantial.

In this work we considered the expansion of the inter atomic force constants up to the third order, and the Hamiltonian is then given by

$$H = U_0 + \sum_i \frac{m\mathbf{p}_i^2}{2} + \frac{1}{2!} \sum_{ij\alpha\beta} \Phi_{ij}^{\alpha\beta} u_i^\alpha u_j^\beta + \frac{1}{3!} \sum_{ijk\alpha\beta\gamma} \Psi_{ijk}^{\alpha\beta\gamma} u_i^\alpha u_j^\beta u_k^\gamma \quad (1)$$

where U_0 corresponds to the ground state energy at the equilibrium atomic positions, \mathbf{p}_i is the momentum vector, indices (i, j) denote atoms in the unit cell, (α, β, γ) are

directions along the cartesian axes and u_i^α is the atomic displacement for atom i along Cartesian direction α . Φ and Ψ are the second- and third-order force constants. The force constant matrices are determined through a minimization procedure of the differences in forces between the model Hamiltonian and AIMD calculations. Symmetries in the force constant matrices have been fully taken into account by considering the symmetry group of the InSb crystalline phase. For force constants fit to AIMD at a given T_{MD} the third order force constants can be used perturbatively to calculate different thermodynamic quantities described below. Here temperature also enters, through Bose Einstein occupations, which allows for an estimation of the separate effects of T on the force constants and the occupation numbers.

The thermal conductivity tensor is given by

$$\kappa^{\alpha\beta} = \frac{1}{(2\pi)^3} \sum_s \int d\mathbf{q} C_\lambda v_{\lambda\alpha} v_{\lambda\beta} \tau_{\lambda\beta}, \quad (2)$$

where C_λ is the contribution per mode $\lambda = (s, \mathbf{q})$ to specific heat, v_β is the phonon velocity, τ_β is the scattering time and α and β are cartesian components.

The scattering times are calculated from a full inelastic phonon Boltzmann equation (PBE) given by:

$$k_B T \mathbf{v}_\lambda \cdot \nabla T \frac{\partial n_{0\lambda}}{\partial T} = \sum_{\lambda'\lambda''} \left[W_{\lambda\lambda'\lambda''}^+ (\Psi_{\lambda''} - \Psi_{\lambda'} - \Psi_\lambda) + \frac{1}{2} W_{\lambda\lambda'\lambda''}^- (\Psi_{\lambda''} + \Psi_{\lambda'} - \Psi_\lambda) \right] \quad (3)$$

where the left hand side represents the phonon diffusion induced by thermal gradient ∇T , $n_{0\lambda} \equiv n_0(\omega_\lambda)$ is the equilibrium phonon distribution function. The right hand side corresponds to the collision term for three phonon interactions. \mathbf{v}_λ is the phonon velocity in mode λ and $W_{\lambda\lambda'\lambda''}^\pm$ are three-phonon scattering rates. Equation (3) is solved using a single iteration of the approach described in Ref.[9] (i.e. the lifetimes are calculated using equilibrium Bose Einstein occupations).

The linear thermal expansion coefficient, α , can be obtained by a sum of the $\gamma_s(\mathbf{q})$ over all modes, weighted by the mode specific heat:

$$\alpha = \frac{B_T}{(2\pi)^3} \sum_s \int d\mathbf{q} C_\lambda \gamma_\lambda, \quad (4)$$

where B_T is the isothermal compressibility and γ_λ is the Mode Gruneisen parameter.

3. Computational Details

The density functional theory (DFT) calculations were performed using the VASP code [10], within the generalized gradient approximation (GGA) by Perdew, Burke and Ernzerhof revised for solids (PBEsol) [11] and projector augmented wave (PAW) implementation[12, 13]. The valence electron configurations of $5s^2 5p^1$ and $5s^2 5p^3$ are considered for In and Sb, respectively. The cutoff energy of plane wave basis set is 350 eV and the electronic energy convergence was kept to values within 10^{-8} eV.

The optimized lattice constant is 6.49 Å, which is in excellent agreement with the experimental value of 6.48 Å[14]. For the *ab initio* molecular dynamics, we used a time step of 1 fs with PBEsol and a *Langevin* thermostat (PS-L) at 300 K. The *Berendsen* thermostat (PS-B) was also considered to evaluate the sensitivity of our predictions to different thermostats. Along the same lines, we have also considered the Armiento-Mattsson 2005 exchange correlation functional (AM05)[15] with both Berendsen (AM05-B) and Langevin (AM05-L) thermostats. Newton’s equations of motion were integrated using the Verlet algorithm [16]. A 54-atom supercell ($3\times 3\times 3$ of the fcc unit cell) for the AIMD simulations was considered, and a 128-atom supercell ($4\times 4\times 4$) was used to study the size effect for few particular calculations. The lattice thermal conductivity and linear thermal expansion is calculated with numerical integration on a $25\times 25\times 25$ Monkhorst-Pack[17] q -point grid to ensure convergence.

4. Results

4.1. Phonon band structure

Our calculated phonon spectra (including LO-TO splitting) at 300 K are shown in Fig. 1, together with experimental data [19, 20, 18]. Detailed comparison at high-symmetry points are listed in Table 1. For the acoustic phonons, the volume variation of $\pm 1\%$ and using different xc-functional/thermostat (PS-B, PS-L, AM05-B and AM05-L) has relatively little effect except around the X and K points, and excellent agreement is obtained in comparison with measured data. On the other hand, the calculated phonon frequencies of the optical branches are underestimated. The volume effect on the optical modes is larger than that for the acoustic modes. The volume variation causes mainly a constant shift in frequencies, such that the phonon velocities would remain similar. Using a different xc-functional (AM05 compared with PS) shows insignificant effect around zone boundaries (X, K and L), but is more visible (higher frequencies from AM05) near the Γ -point. This implies that the xc-functional has more subtle influence than merely affecting the equilibrium volume. The phonons appear well converged with respect to supercell size.

4.2. Anharmonic effects

The lattice anharmonicity is manifested in various ways. In this paper we focus on two prominent properties, viz. the thermal expansion coefficient and the lattice thermal resistivity. Fig. 2(a) shows our calculated temperature dependence of the linear thermal expansion coefficient (TEC), compared with measurement.[21, 22] The TEC of InSb is negative below ~ 60 K, and in this temperature range our predictions are in good agreement with experimental data. The curves which are a bit further from experiment are a) the compressed volume (PS-B with $a_0-1\%$), which shows a strong effect of pressure, and b) the AM05-L with experimental a_0 and a $3\times 3\times 3$ supercell, which shows anharmonic properties are more sensitive to xc effects. At higher temperatures, the

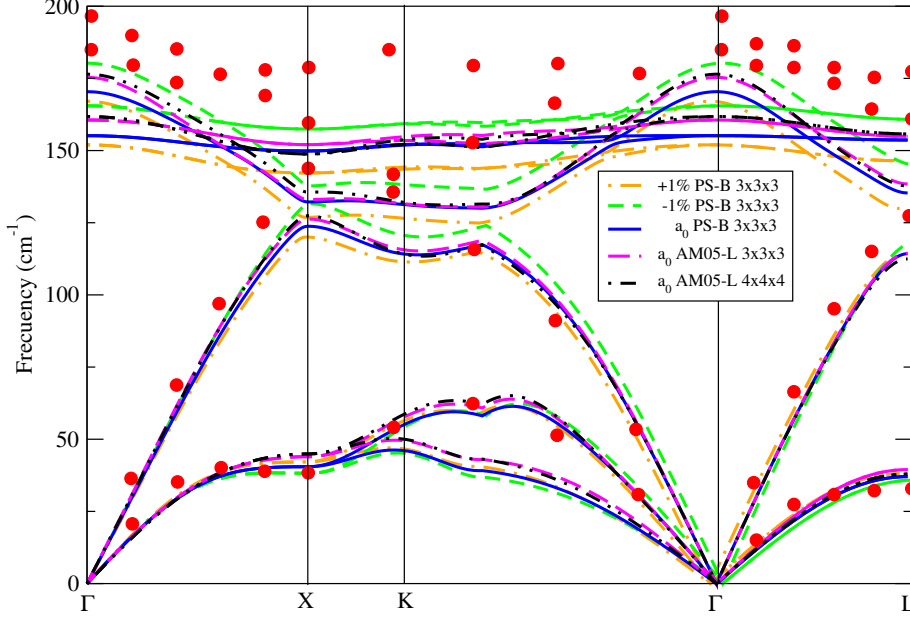


Figure 1. (Colour online). Phonon dispersion curves of InSb along high symmetry directions. The calculated curves are derived from MD run at 300 K and a $3 \times 3 \times 3$ supercell, using PBEsol-Berendsen (PS-B) with the experimental lattice constant $a_0 = 6.48 \text{ \AA}$, $a_0 + 1\%$ and $a_0 - 1\%$; the AM05 xc-functional with Langevin thermostat (AM05-L); as well as AM05-L for a $4 \times 4 \times 4$ supercell with the experimental a_0 . Experimental data are shown as dots from Ref. [18].

calculated TECs show significant underestimation, in particular the AM05-L with a_0 and $3 \times 3 \times 3$ supercell which stays mostly negative up to 300 K. For higher temperatures one

As an intrinsic semiconductor, the thermal conductivity of InSb is mainly contributed by lattice vibrations, limited by anharmonic phonon-phonon scatterings. The thermal resistivity $1/\kappa_l$ shows a linear temperature dependence from 100 to 400 K, which originates from the linear dependency of phonon occupation number on temperature. The temperature dependent theoretical thermal resistivities are in good agreement with experimental values [6] (Fig. 2 (b)), with moderate discrepancies for PS-B with $a_0 - 1\%$ (overestimation) and AM05-L with a_0 and $4 \times 4 \times 4$ supercell (underestimation). As the measured $1/\kappa$ includes electronic contribution and phonon scatterings with other imperfections, the calculated contribution from phonon-phonon interactions is expected to underestimate, as given by the $4 \times 4 \times 4$ supercell, but this could be compounded by a small xc effect in the equilibrium AM05 volume. The first message is that convergence of the thermal conductivity is slower with respect to the size

Table 1. Phonon frequencies (in cm^{-1}) of InSb at 300 K at high-symmetry points (Γ , X and L points) of the Brillouin zone. (PS=PBEsol, B=Berendsen, L=Langevin)

Mode		PS-B	PS-B	PS-B	PS-L	AM05-L	AM05-B	Expt.
		(a_0)	($a = a_0 + 1\%$)	($a = a_0 - 1\%$)	(a_0)	(a_0)	(a_0)	
Γ	TO	154.9	151.8	165.4	159.8	160.2	154.9	179.9 ^a , 186 ^b , 185 ^c
	LO	170.0	166.8	179.8	174.9	175.2	170.3	192.1 ^a , 198.6 ^b , 197 ^c
X	TO	149.0	142.3	157.0	151.1	152.1	149.0	181.4 ^b , 179.5 ^c
	LO	131.8	126.9	137.8	132.9	133.2	132.9	163.4 ^b , 158.4 ^c
	TA	40.1	42.2	37.2	42.9	44.6	41.5	38.6 ^b , 37.4 ^c
	LA	123.4	119.6	131.5	126.6	125.2	124.5	143.4 ^c
L	TO	153.5	146.2	160.5	154.9	154.6	152.8	179.8 ^b , 177.1 ^c
	LO	135.0	129.7	144.8	138.5	138.1	134.6	165.0 ^b , 160.8 ^c
	TA	36.2	38.0	35.5	38.0	39.4	38.0	33.8 ^b , 32.7 ^c
	LA	113.6	113.7	118.2	111.9	114.7	114.2	127.1 ^c

^aRef.[19](T = 293 K)

^bRef.[20] (T = 20 K)

^cRef.[18] (T = 300 K)

of the supercell. For both TEC and κ_l , the results from AM05-L no longer lie between those for PS-B with a_0 and $a_0-1\%$, as is the case for phonon dispersion. This shows again that the effect of the xc functional on the anharmonicity is not merely a volume effect.

5. Conclusions

In summary, combining DFT-based molecular dynamics and the TDEP method, we have studied the harmonic and anharmonic lattice vibrational properties of InSb, from calculated temperature dependent second and third order force constants. The calculated lattice thermal resistivity is in fair agreement with experimental data, whereas our prediction underestimates TEC at high temperature. This disagreement needs to be checked by considering other effects such as thermal expansion or different pseudopotentials. In general, we also provide quantitative evaluations of the effects of the xc-functional, thermostat, volume and size of the supercell.

Acknowledgments

Support from the Knut & Alice Wallenberg Foundation (KAW) project ‘‘Isotopic Control for Ultimate Material Properties’’ and the Swedish Foundation for Strategic Research (SSF) program SRL10-002 is gratefully acknowledged. Supercomputer resources were provided by the Swedish National Infrastructure for Computing (SNIC). This work used the Extreme Science and Engineering Discovery Environment (XSEDE), which is

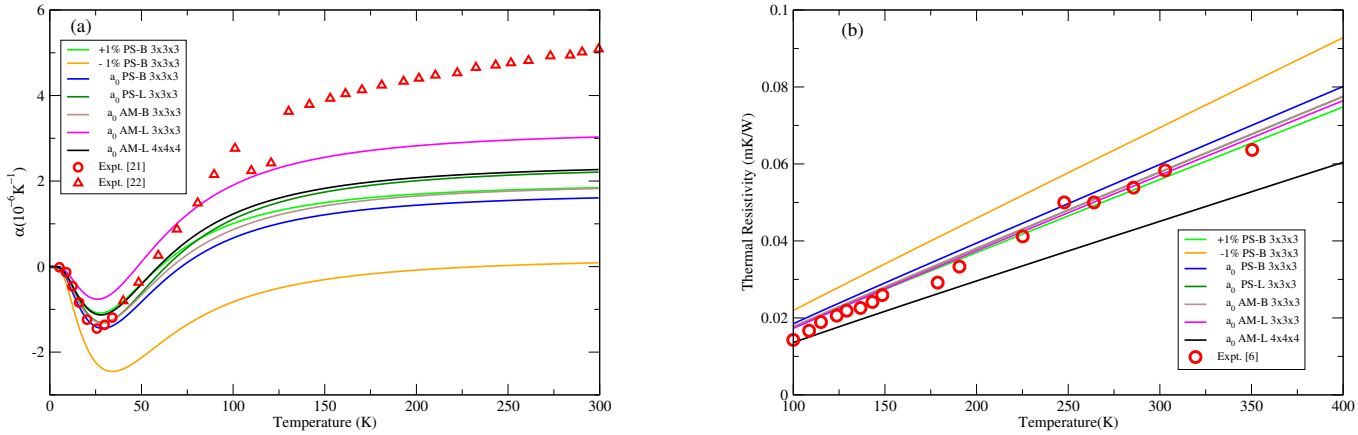


Figure 2. (Colour online) All calculations are based on force constants from MD at $T=300$ K. (a) Calculated linear thermal expansion coefficient for InSb as a function of temperature up to 300 K, compared with experimental data (red circle[21] and triangle[22]). Results with supercell $3\times 3\times 3$ with PBEsol functional and different thermostat: Berendsen and Langevin, the AM05 with thermostat Berendsen curves; the AM05 functional and Langevin thermostat (AM05-L) supercell $3\times 3\times 3$ and supercell $4\times 4\times 4$ curves. Include curves PS-B with +1% and -1%. (b) Calculated and measured [6] thermal resistivity as a function of temperature. Theoretical results include PS-B, PS-L, AM05-B and AM05-L with a_0 . Include $a_0+1\%$, and $a_0-1\%$. AM05-L with supercell $4\times 4\times 4$ at a_0 .

supported by National Science Foundation grant number OCI-1053575 and the Super Computing Systems (Mountaineer and Spruce) at WVU, which are funded in part by the National Science Foundation EPSCoR Research Infrastructure Improvement Cooperative Agreement 1003907, the state of West Virginia (WV EPSCoR via the Higher Education Policy Commission) and WVU. A.H. Romero acknowledge the support of the Marie Curie Actions from the European Union in the international incoming fellowships (grant PIIFR-GA-2011-911070) and the Donors of the American Chemical Society Petroleum Research Fund for partial support of this research under contract 54075-ND10. MJV acknowledges an ARC grant (TheMoTherm # 10/15-03) from the Communauté Française de Belgique, and computer time from CECI, SEGI, and ThermoSpin on ARCHER (3IP FP7 RI-312763). ALM acknowledges a SDRE grant from the University of Liège and support from CONACyT of México.

References

- [1] Zebarjadi M, Esfarjani K, Dresselhaus M S, Ren Z F and Chen G 2012 *Energy Environ. Sci.* **5** 5147
- [2] Cahill D G and Pohl R O 1988 *Annual Review of Physical Chemistry* **39** 93
- [3] Rode D L May 1971 *Phys. Rev. B* **3** 3287

- [4] Mingo N 2004 *Appl. Phys. Lett.* **84** 2652
- [5] Jaworski C, Myers R, Johnston-Halperin E and Heremans J 2012 *Nature* **487** 210
- [6] Holland M G Apr 1964 *Phys. Rev.* **134** A471
- [7] Hellman O, Abrikosov I A and Simak S I Nov 2011 *Phys. Rev. B* **84** 180301
- [8] Hellman O and Abrikosov I A Oct 2013 *Phys. Rev. B* **88** 144301
- [9] Broido D A, Ward A and Mingo N Jul 2005 *Phys. Rev. B* **72** 014308
- [10] Kresse G and Furthmüller J Oct 1996 *Phys. Rev. B* **54** 11169
- [11] Perdew J P, Ruzsinszky A, Csonka G I, Vydrov O A, Scuseria G E, Constantin L A, Zhou X and Burke K Apr 2008 *Phys. Rev. Lett.* **100** 136406
- [12] Kresse G and Hafner J Nov 1993 *Phys. Rev. B* **48** 13115
- [13] Kresse G and Furthmüller J 1996 *Computational Materials Science* **6** 15
- [14] Straumanis M E and Kim C D 1965 *Journal of Applied Physics* **36** 3822
- [15] Mattsson A E, Armiento R, Paier J, Kresse G, Wills J M and Mattsson T R 2008 *The Journal of Chemical Physics* **128**
- [16] Verlet L Jul 1967 *Phys. Rev.* **159** 98
- [17] Monkhorst H J and Pack J D Jun 1976 *Phys. Rev. B* **13** 5188
- [18] Price D L, Rowe J M and Nicklow R M Feb 1971 *Phys. Rev. B* **3** 1268
- [19] Lockwood D, Yu G and Rowell N 2005 *Solid State Communications* **136** 404
- [20] Koteles E S, Datars W R and Dolling G Jan 1974 *Phys. Rev. B* **9** 572
- [21] Sparks P W and Swenson C A Nov 1967 *Phys. Rev.* **163** 779
- [22] Gibbons D F Oct 1958 *Phys. Rev.* **112** 136